

Development of self-charging unmanned aerial vehicle system using inductive approach

Khairul Kamarudin Hasan¹, Shakir Saat², Yusmarnita Yusop², Md Rabiul Awal³

¹School of Electrical Engineering, College of Engineering, Universiti Teknologi MARA Cawangan Johor, Johor, Malaysia

²Centre of Telecommunication Research and Innovation, Faculty of Electronic and Computer Engineering, Universiti Teknikal Malaysia Melaka, Melaka, Malaysia

³Department of Electrical Engineering, Universiti Malaysia Terengganu, Terengganu, Malaysia

Article Info

Article history:

Received Mar 30, 2022

Revised Jun 3, 2022

Accepted Jun 21, 2022

Keywords:

Class E amplifier

Inductive approach

Self-charging

Unmanned aerial vehicle

Wireless power transfer

ABSTRACT

This paper presents an alternative approach to power up unmanned aerial vehicle (UAV) system using inductive approach. The main issue of utilizing UAV in any application especially in precision agriculture is the lifetime of the battery. This limits the flight time of the UAV which makes the system is unable to be efficiently applied for precision agriculture purpose. Hence, this paper proposes a new approach of powering UAV system by using so called inductive power transfer (IPT) technology. Through this approach, the system can be powered up wirelessly with no physical link in between transmitter and receiver. To be specific, class E inverter circuit has been designed together with impedance matching circuit to ensure higher efficiency is obtained. Finally, a prototype of IPT system for powering up the UAV system was successfully developed, which is able to transmit 23.32 W of power at 1 MHz operating frequency from 12 V input supply. The system achieved up to 95.73% efficiency.

This is an open access article under the [CC BY-SA](https://creativecommons.org/licenses/by-sa/4.0/) license.



Corresponding Author:

Shakir Saat

Centre of Telecommunication Research and Innovation, Faculty of Electrical and Computer Engineering
Universiti Teknikal Malaysia Melaka (UTeM)

76100 Durian Tunggal Melaka, Malaysia

Email: shakir@utem.edu.my

1. INTRODUCTION

Wireless power transfer (WPT) is the transmission of energy without any physical link between the device and the power source. Without the interconnecting of wires or cables, WPT accomplished energy transmission by creating an electromagnetic field, or electric field or magnetic field between the device and the power source [1]. By using WPT technology, the charging system of electrical devices is innovating and improving with low risk of electric shock, ease of installation as the requirement of adaptor plug-in and out is the refrain, or short circuit and damaged of cables would never exist [2]-[4].

Inductive power transfer (IPT) is the transmission of power in between two coils through a magnetic field. Alternating current (AC) moves through the primary coil which acts as a transmitter, a circular magnetic field creates around the coil by ampere's law [5]. Wire bending in the form of a coil amplifies the magnetic field and the more loops the coil makes, the larger the field creates. Then, the magnetic field transmits to the secondary coil which acts as a receiver, where the coil induces an alternating electromagnetic field (EMF) by following Faraday's law of induction, which alters the EMF to AC in the receiver [1]-[5]. The induced AC may either be powering up the device directly, or the AC will go through a rectifier to transform back into DC to fulfill the requirement of the load. IPT is widely used in current commercial products,

because of high efficiency, low cost, and still able to function at the extreme condition of the environment as IPT will not be affected by water or dust [6].

Unmanned aerial vehicles (UAVs) or also commonly known as drones, have been used in many different applications since a few years ago such as in maintenance, transportation, delivery and military industry [7], [8]. In fact, researchers are discovering all sorts of ingenious ways to improve efficiency and maximize profit using UAV technology. However, the main issue using UAV in any application especially in agriculture is the limitation of its battery life-time that limits its flight time. This is true as the depletion of the onboard supply is very significant as the amount of power needed by the motors is very large. Due to this, the UAVs require a frequent charge to allow the system to be used at a longer time operation and normally it involves direct human intervention [9], [10].

To overcome the issue, many researchers have devoted their time to focus on the autonomous charging approach to increase the endurance and the overall flight time as given in [11], [12]. As highlighted in [10], Silverman *et al.* [13] demonstrated the autonomous recharging on a charging dock for a ground robot and researchers in [14] proposed a battery swapping station approach for small co-axial helicopters. The recent work on contact-based technique can be found in [11] which is able to improve the misalignment issue and also the efficiency of the system. However, despite of many results available in the framework of contact-based autonomous charging approaches, every of the results suffer from their own conservatisms. In fact, the contact-based approach requires a perfect landing on the charging stations, and this is hard to achieve in the outdoor environment. Also, the method needs to have a reliable mechanical design and structure to ensure the perfect bond of the electrodes for good conductivity, which eventually increases the control complexity and cost [10].

Due to the above problems of contact-based autonomous charging approach, a more reliable solution has been proposed by [10] by utilizing WPT approach. A comprehensive survey on the UAVs solutions for increasing the flight time based on the WPT approach can be found in [15]. Chittoor *et al.* [15] have deliberated in details the available approaches of the wireless autonomous charging and mainly focus on the near-field techniques (such as capacitive, inductive and magnetic resonant approach) for efficient power transfer of less than one meter and far-field techniques (such as laser-based charging and microwave-based charging) for long-range power transmission. Most of the recent works focused on the near-field approach as the far-field approach has always been associated with the human safety issue and therefore the practicality of the approach is questionable. The inductive approach provides a better solution in term of overall output efficiency and reliability than its counterpart, i. e. capacitive approach [16], [17]. Thus, in this work, a wireless charging system for UAV system based on the inductive approach is proposed.

In contrast with [10], our work utilizes the class E inverter and impedance matching circuits to improve the efficiency of the system by ensuring the switching loss is minimal. The contribution of this work lies in the development of autonomous charging based on IPT system using class E inverter with impedance matching circuit that is able to transmit 23.32 W power to the load with efficiency of 95.73% at 1 MHz operating frequency. This paper is organized as follows: Research method is given section 2. Section 3 presents the results and discussion of the work in detail. Then, the conclusion is provided section 4.

2. RESEARCH METHOD

This session explains the research design and procedures required in order to design IPT system, Class E inverter, and impedance matching circuit for the wireless autonomous charging UAV system.

2.1. Class E inverter design

The class E circuit is shown in Figure 1. The specification used in designing the circuit is given in Table 1. The operation of class E inverter is regarded on the theory that the MOSFET acts as a switch to undergo zero voltage switching (ZVS) and convert the DC voltage to AC. Class E inverter is popular and commented to use due to its inherent robust, simple in design, and theoretically produces a 100% efficiency [18], [19]. In order to design class E inverter, the components should be first calculated using equations that are listed in [19]. From the values obtained, the type of MOSFET can then be decided. Apart from that calculated values, the voltage at gate (of MOSFET), V_g , must also be considered because it will directly affect the drain voltage, V_d , as the V_d is three times larger than V_g . So, the minimum input for V_g needs to be lower enough to ensure the resonant tank is in good operation condition. In the meantime, the DC power supply has been used to power up the class E inverter.

For the resonant tank, some important components such as series inductor (L_o), series capacitor (C_o), and shunt capacitor (C_s) need to be calculated. The theoretical calculation for these components is adapted from [19]. Hence, the load resistance, R can be determined by using (1).

$$R = R_s = \frac{8V_{dc}^2}{(\pi^2+4)P_o} = 0.5768 \frac{V_{dc}^2}{P_o} \quad (1)$$

Then, by assuming quality factor, $Q_L = 10$, the sinusoidal waveform of the current will go through the resonant circuit. using (2), (3), and (4), the value of C_s , L_o , and C_o are calculated as,

$$L_o = \frac{Q_L R}{\omega} \quad (2)$$

$$C_o = \frac{8}{\pi(\pi^2+4)\omega R} \quad (3)$$

$$C_s = \frac{1}{\omega R \left[Q_L - \frac{\pi(\pi^2-4)}{16} \right]} \quad (4)$$

Furthermore, the choke inductor, L_c is assumed to be high enough so that the AC ripple on the full-load dc supply input current, I_l can be negligible. Thus, the value of L_c must be greater than the value obtained in (5).

$$L_c = 2 \left(\frac{\pi^2}{4} + 1 \right) \frac{R}{f} \quad (5)$$

Based on (1) to (5), the obtained components values are given in Table 2. Then, the simulation of class E circuit is built in MATLAB/SIMULINK as shown in Figure 2. For this simulation design, the value of series capacitor and shunt capacitor have to be tuned in order to get the output voltage value that is almost similar to the theoretical value in order to obtain the perfect ZVS condition. This is to ensure the switching losses is zero theoretically as highlighted in (19). Once the simulation results are good (see the results in section 3), then, the experimental work is carried out. The circuit is shown in Figure 3.

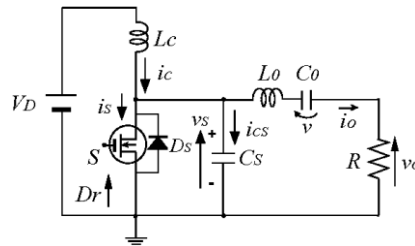


Figure 1. Basic structure of class E inverter

Table 1. Specification for class E inverter

Parameters	Value
Frequency, f	1 MHz
Duty cycle, D	0.5
Input Voltage, V_D	12 V
Quality factor	10
Output power	24.5 W

Table 2. Theoretical values for class E inverter

Parameters	Symbol	Value	Unit
Choke inductor	L_c	23.51	μH
Series capacitor	C_o	5.3016	nF
Series inductor	L_o	5.3956	μH
Shunt capacitor	C_s	8.6193	nF

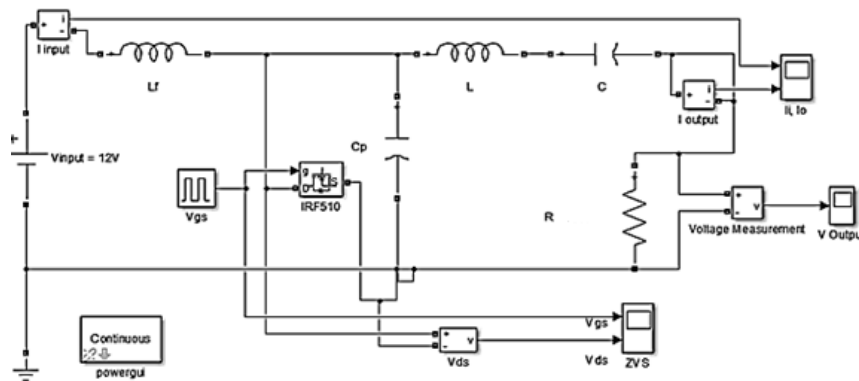


Figure 2. Class E inverter circuit built in MATLAB/Simulink

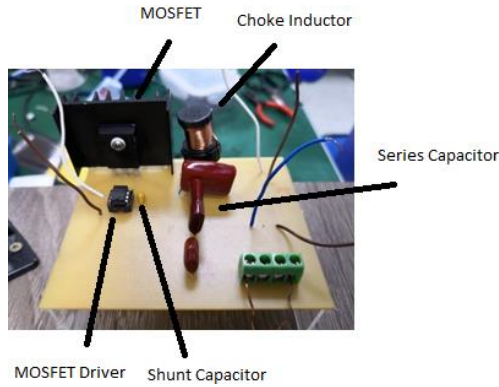


Figure 3. Fabricated class E inverter circuit

2.2. Impedance matching circuit

IPT system utilizes inductor coils to transfer power wirelessly from transmitter to load. These coils create the induced currents and increases the volt-ampere (VA) rating from the power source, when high operating frequency is generated through the coils. The impedance matching circuit is normally added in the circuit to provide maximum power transfer between the source and its load. The impedance matching circuit is added before the resistive load and according to [19], they are four types of impedance matching circuit which are series-series, series-parallel, parallel-series, and parallel-parallel as shown in Figure 4 [20]. Series-series impedance matching network has been chosen here due to its ability to increase the current and therefore the output power can be enhanced. This is true as the solution allows the resonant frequency to operate at the frequency between f_{01} shown in (6) and f_{02} shown in (7) in order to absorb maximum power received and improve efficiency of the system [21], [22].

The value of series capacitor used for impedance matching network is calculated using (9) by applying receiver coil inductor value and operating frequency to the equation. The experimental work for impedance matching and rectifier circuit has been constructed on polychlorinated biphenyl (PCB) as shown in Figure 5.

$$f_{01} = \frac{1}{2\pi\sqrt{LC}} \quad (6)$$

$$f_{02} = \frac{1}{2\pi\sqrt{LC_{eq}}} \quad (7)$$

$$C_{eq} = \frac{C \times C_1}{C + C_1} \quad (8)$$

$$f_r = \frac{1}{2\pi\sqrt{LC}} \quad (9)$$

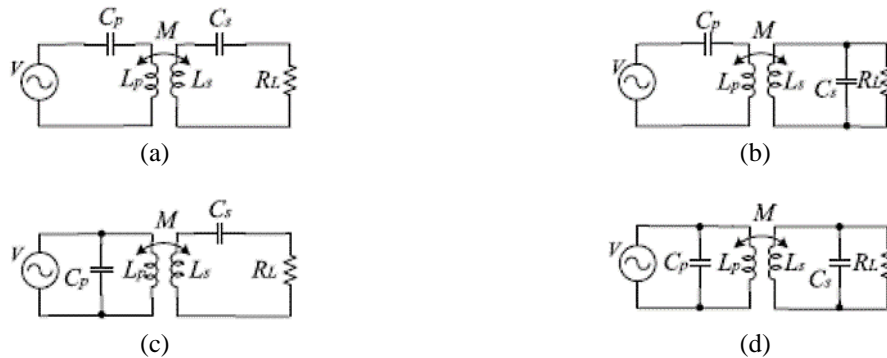


Figure 4. Types of impedance matching network to improve the efficiency of IPT system:
 (a) series-series (SS), (b) series-parallel (SP), (c) parallel-series (PS), and (d) parallel-parallel (PP).
 Circuit in (a) is used in this work

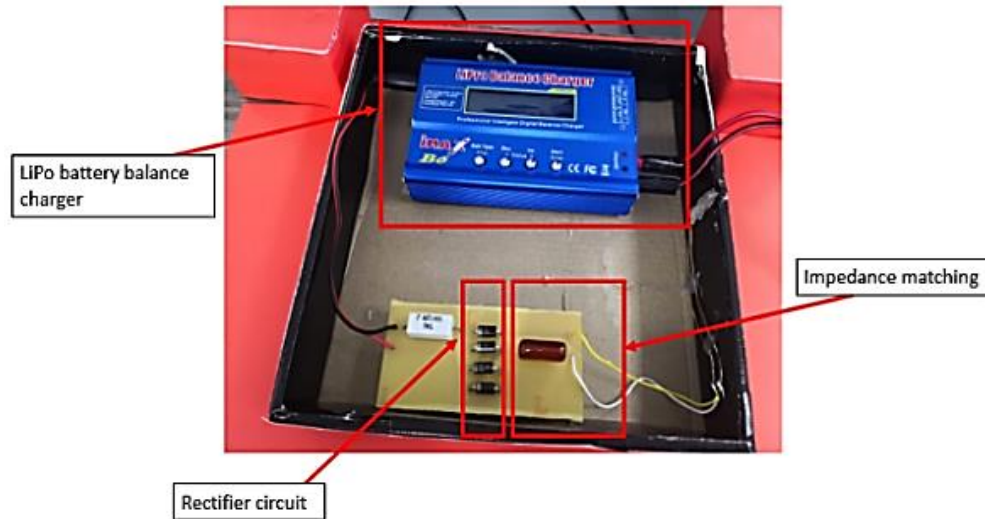


Figure 5. Receiver part for the prototype

3. RESULTS AND DISCUSSION

In this part, the results and data obtained for this work are presented and explained in details.

3.1. Class E inverter and impedance matching circuit

Table 3 shows the comparison between the simulation and experimental values of the class E inverter with impedance matching circuit. The difference is mainly due to the availability of the practical components values in market. To note here as well that the inductor at the resonant tank (used in the simulation) is replaced with a transmitting coil (for experiment purpose). According to the simulation result shown in Table 3, the voltage across drain to source, V_{ds} at off state is 42.54 V. Hence, MOSFET IRF250 is chosen for class E inverter circuit as a switching device, because of its ability to perform fast switching and able to handle such voltage. Due to the capacitance values for the shunt capacitor and series capacitor that were used in the simulation are not available practically, hence, two different values of capacitor are combined to obtain the nearest value for experimental work.

Table 3. Result comparison between simulation and experimental value

Parameters	Simulation Value	Practical value	Unit	Difference (%)
R	3.50	5.00	Ω	30.00
Lc	30.00	45.00	μH	33.33
C_1	9.30	9.40	nF	1.06
L	5.50	11.50	μH	52.17
C	5.30	2.29	nF	56.79
I_{DC}	1.99	2.03	A	1.97
$V_{ds}(\text{peak, off})$	42.54	36.00	V	15.37
V_{gs}	5.00	5.00	V	0.00
$V_{o, m(\text{peak})}$	12.35	12.71	V	2.83
$V_{o, rms}$	16.65	17.13	V	2.80
$I_{o, m(\text{peak})}$	3.70	3.60	A	0.81
$I_{o, rms}$	2.37	2.59	A	8.49
P_i	23.88	24.36	W	1.97
P_o	22.84	22.87	W	1.31
η	95.67	93.91	%	1.83

The simulation result for class E converter circuit is shown in Figure 6. We can see that the ZVS condition is well achieved in this work. When the voltage at the V_g drops to zero, the voltage at V_d is achieving the value of 42.51 V which means there is a flow of voltage while the MOSFET is in off state.

In comparison to the theoretical value which is 42.74 V, the simulation result is 0.47% lower than the calculated value. When the switch voltage has reached maximum value and dropped to negative with the time interval, the MOSFET is switched on. During ON-state, the voltage across drain to source in simulation result is 0.3894 V.

Therefore, to reduce the switching losses during the on-state, a lower value of on-state resistance, r_{ds} , MOSFET must be considered in the design. The power absorbed by the MOSFET is directly proportional to the r_{ds} , and switching current. So, when the r_{ds} decreases, the on-voltage is also reduced. At the same time, the power absorbed by the MOSFET is reduced and the output power of the class E inverter is improved. At the early stage of the work, MOSFET IRF512 was chosen to construct the class E inverter, because it is cheaper and less bulky compare to IRF250. However, MOSFET IRF512 has a higher value of on-resistance value which is 0.8Ω compare to IRF250 which is only 0.085Ω . IRF512 has reduced the theoretical value of efficiency for class E inverter from 99.99% to 76.26%.

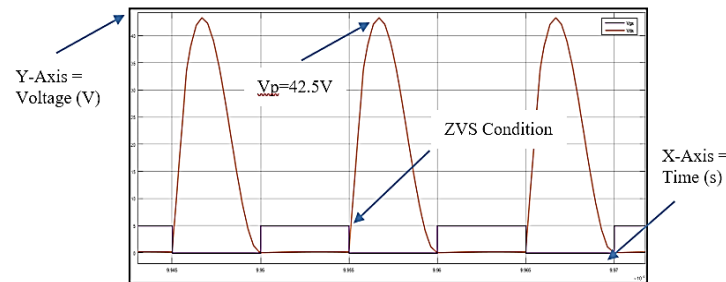


Figure 6. ZVS simulation result

The simulated result of output current and output voltage as shown in Figure 7 and Figure 8, respectively. The output voltage for class E inverter is AC voltage and simulated result was firstly obtained in root mean square value. Then, the peak value for output voltage is calculated using (10) and the value is 12.35 V, which is 2.83% differs from the calculated one.

$$V_{rms} = 0.707 \times V_{max} \quad (10)$$

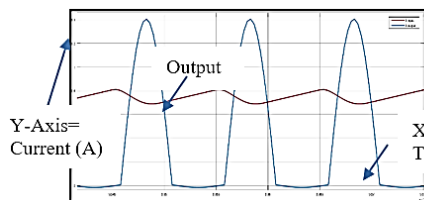


Figure 7. Output current for simulation

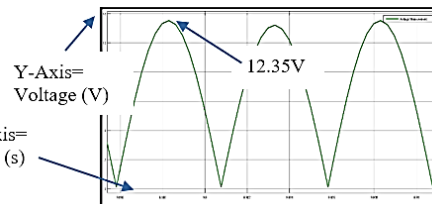


Figure 8. Output voltage for simulation

The simulated input power is calculated by $P_I = I_{dc} \times V_I$ which gives 23.88 W and the output power is calculated by $P_o = V_{rms} \times I_{rms}$ which gives 22.84 W. Efficiency of simulated result for the class E inverter is calculated by $\eta = \frac{P_o}{P_I} \times 100\%$ and yield 95.67% efficient. Figure 9 shows the ZVS waveform in the experimental work. When the MOSFET is in on-state, the V_{gs} is represented as rectangular waveform with the value of 5 V and each decade in y-axis from the graph equal to 2 V. At the off-state, the V_{ds} is represented as sinusoidal waveform and the value is 36 V with each decade of the y-axis in the graph equal to 5 V. For this class E inverter circuit, the obtained peak voltage, $V_{o,m}$ is 12.71 V. The difference between the theoretical value and practical value is 2.83%. Next, the output current result is also obtained and shown in Figure 10. The output current is obtained in AC waveform as the inductor needs an AC current to induce electromagnetic field for power transmission. The theoretical output current is 2.7% lower than the calculated value. Input power and output power are the essential parameters to obtain the efficiency of the designed system. The experimental input power and output power for class E inverter is $P_i=24.36$ and $P_o=22.87$. Convert into the efficiency, the class E inverter reached up to 93.91%. The power losses is mainly due to the fast switching operation which generated heat at MOSFET. On the other hand, the internal resistance from each of the components such as RLC series circuit, C_1 and L_s are also contributed to the power losses.

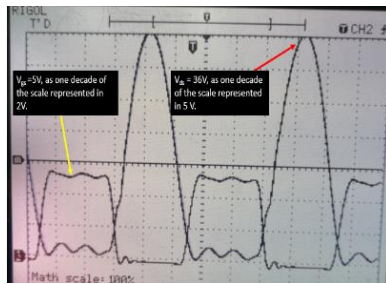


Figure 9. ZVS practical result

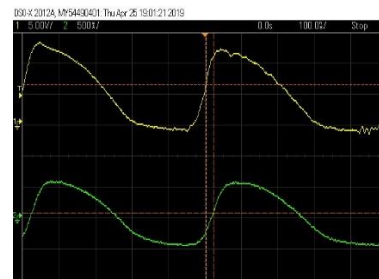


Figure 10. Output current practical result

3.2. Analysis on distance and misalignment variations between transmitter and receiver coil

This part intends to study on the maximum distance between transmitter (charging platform) and the receiver (UAV power supply). This is important to ensure the perfect design can be made at both transmitter and receiver to obtain the highest efficiency of the power transmission. The distance between transmitter coil and receiver coil has been varied as shown in Figure 11. The transmitter coil is placed under the table which act as charging tower for UAV wireless charging system and the receiving coil is placed under the box which carried by the UAV and connected with the rectifier circuit and DC voltage is supplied to the battery charger as shown in Figure 12.

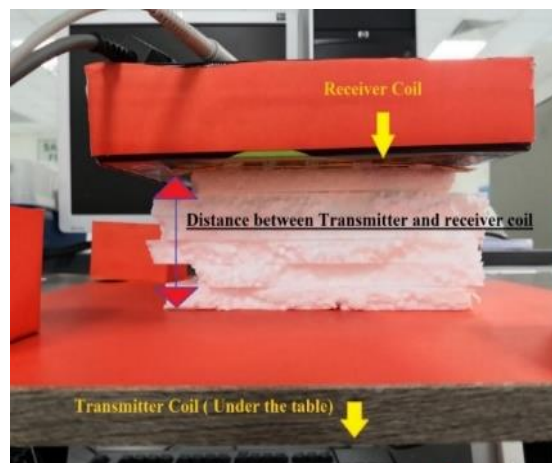


Figure 11. Distance analysis between receiver and transmitter coil

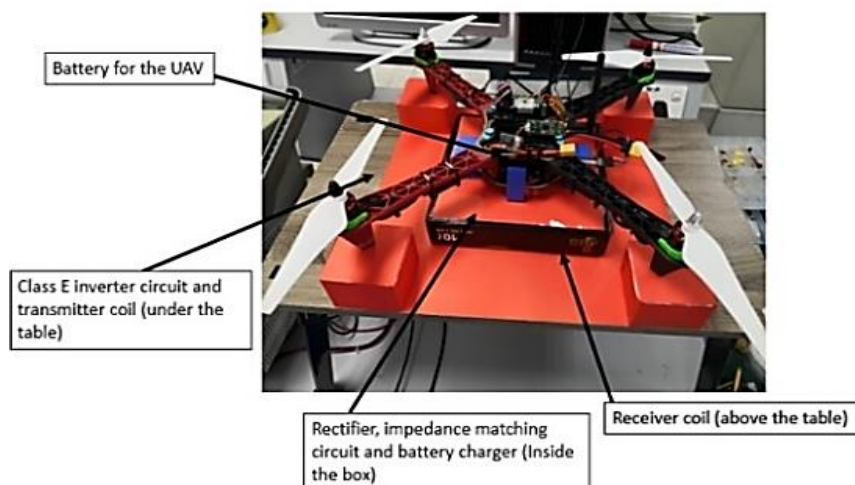


Figure 12. Completed prototype for UAV wireless

Table 4 shows the result at each distance separation from 3 cm (the thickness of the table) to 8cm. According to the experimental result, the highest efficiency is 93.91% (when the Tx coil and Rx coil are at nearest distance with each other). However, the lowest efficiency which is 8.65% is when the Tx coil and Rx coil is apart with each other for 8 cm. From the experiment, the charger was failed to power up the UAV when the Tx coil and Rx coil is more than 6 cm apart.

Table 4. Analysis of efficiency on the distance

Distance (cm)	Voltage (V)	Current (A)	P _o	P _i	Efficiency, η (%)
3	12.71	3.60	22.87	24.36	93.91
4	12.05	3.11	18.74	24.36	76.92
5	11.7	2.64	15.44	24.36	63.40
6	11	1.17	6.44	24.36	26.42
7	8.6	0.96	4.13	24.36	16.95
8	6.8	0.62	2.11	24.36	8.65

The mutual coefficient depends on the mutual flux between the Tx coil and Rx coil. Thus, the matching condition can be found easily, by adjusting the position of the loop to modify the input impedance. Without matching, the efficiency of the system decreases rapidly as the misaligned distance increases [23]-[25].

Next, we focus on the efficiency results when the Tx coil and Rx coil is misaligned with each other and the experimental result is recorded in Table 5. The result was recorded when the Rx coil is moved horizontally away from the Tx coil in every 2 cm as shown in Figure 13. The efficiency reached at 93.91% when the Tx coil and Rx coil is almost perfectly aligned with each other. However, the lowest efficiency is 18.47% with the misaligned distance of 10 cm. At 10 cm distance, the Rx coil almost away from the range of Tx coil. Therefore, the Rx coil is not able to resonate at the operating frequency.

Figure 14 shows the ZVS graph of the Rx coil that is 10 cm away from the Tx coil. The input impedance is varied along with the coupling coefficient between the Tx coil and Rx coil. Through this ZVS result, it is obvious that the efficiency will drop significantly once the misalignment occurs.

Table 5. Analysis of efficiency on misalignment

Distance (cm)	Voltage (V)	Current (A)	P _o	P _i	Efficiency, η (%)
0	12.71	3.67	23.32	24.36	95.74
2	12.03	3.27	19.67	24.36	80.74
4	11.65	3.16	18.41	24.36	75.56
6	11.03	2.58	14.23	24.36	58.41
8	10.5	1.93	10.13	24.36	41.59
10	7.2	1.25	4.50	24.36	18.47

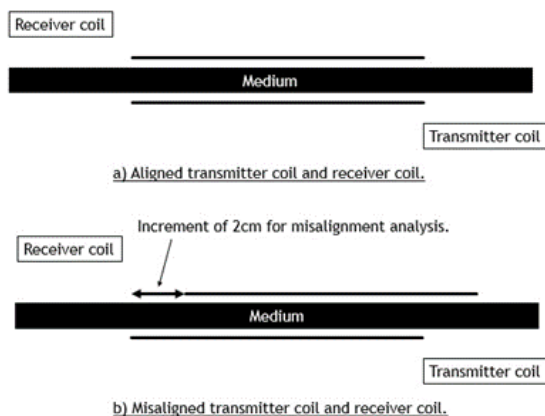


Figure 13. Concept of misalignment analysis

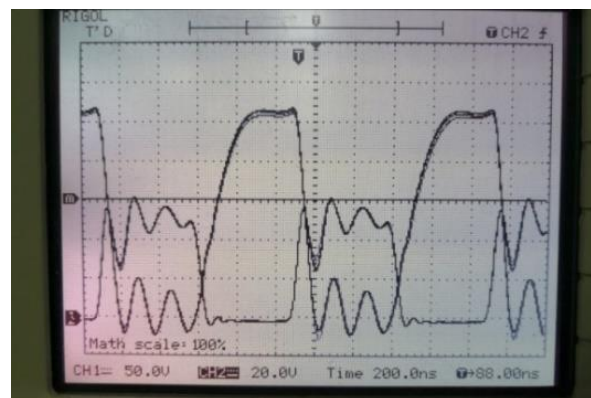


Figure 14. ZVS graph when the TX and Rx coil is misaligned

3. CONCLUSION

In a nutshell, the overall proposed design of IPT system for the UAV charging system is able to transmit 23.32 W of power to the UAV at rectifier circuit by using impedance matching circuit and 18.41 W

power without impedance matching network. Thus, the proposed impedance matching network was successfully produced higher maximum transferrable power. The efficiency of the developed system at aligned condition and at 3 cm distance is 93.91%.

Despite of the success of transmitting the power to the UAV system at a good efficiency, our proposed solution suffers from the efficiency drops when the distance between transmitter and receiver changes. This is also true when the misalignment occurs. Therefore, the future work lies in proposing the control mechanism to stabilize the output power despite variations in the distance or alignment of transmitter and receiver.

ACKNOWLEDGEMENTS

This research was funded by the BESTARI Research Grant Phase 3/2020 of Universiti Teknologi MARA (UiTM) Johor Branch, Malaysia (600-UiTMCJ (PJIA.5/2)) grant. Sincerely to express the appreciation to Universiti Teknologi MARA (UiTM) and Universiti Teknikal Malaysia Melaka (UTeM) for professional support.





REFERENCES

- [1] Z. Zhang, H. Pang, A. Georgiadis, and C. Cecati, "Wireless Power Transfer—An Overview," in *IEEE Transactions on Industrial Electronics*, vol. 66, no. 2, pp. 1044-1058, Feb. 2019, doi: 10.1109/TIE.2018.2835378.
- [2] A. Alphones and P. Jayathurathnage, "Review on wireless power transfer technology (invited paper)," *IEEE Asia Pacific Microwave Conference (APMC)*, 2017, pp. 326-329, doi: 10.1109/APMC.2017.8251445.
- [3] K. Agarwal, R. Jegadeesan, Y. X. Guo, and V. Thakor, "Wireless Power Transfer Strategies for Implantable Bioelectronics," in *IEEE Reviews In Biomedical Engineering*, vol. 10, pp. 136-161, 2017, doi: 10.1109/RBME.2017.2683520
- [4] X. Lu, P. Wang, D. Niyato, D. I. Kim, and Z. Han, "Wireless Charging Technologies: Fundamentals, Standards, and Network Applications," in *IEEE Communications Surveys & Tutorials*, vol. 18, no. 2, pp. 1413-1452, 2016, doi: 10.1109/COMST.2015.2499783.
- [5] E. Sazonov, "Wearable Sensors: Fundamentals, Implementation and Applications," Elsevier Inc, 2nd Edition, United Kingdom: Mara Corner, 2020.
- [6] C. Wang, O. H. Stielau, and G. A. Covic, "Load models and their application in the design of loosely coupled inductive power transfer systems," in *International Conference on Power System Technology. Proceedings*, 2000, pp. 1053-1058 vol.2, doi: 10.1109/ICPST.2000.897166.
- [7] R. Mahony and V. Kumar, "Aerial robotics and the quadrotor," *IEEE Robotics and Automation Magazine*, 2012, doi: 10.1109/MRA.2012.2208151.
- [8] P. Lima, L. Custodio, M. I. Ribeiro, and J. S. Victor, "The RESCUE Project Cooperative Navigation for Rescue Robots," in *Proceedings of the 1st International Workshop on Advances in Service Robotics*, March 2003.
- [9] A. B. Junaid, Y. Lee, and Y. Kim, "Design and Implementation of Autonomous Wireless Charging Station for Rotary-Wing UAVs," *Aerospace Science and Technology*, vol. 54, pp. 253-266, 2016, doi: 10.1016/j.ast.2016.04.023.
- [10] A. Junaid, A. Konoiko, Y. Zweiri, M. N. Sahinkaya, and L. Seneviratne, "Autonomous Wireless Self-Charging for Multi-Rotor Unmanned Aerial Vehicles," *Energies*, vol. 10, no. 803, pp. 2-14, 2017, doi: 10.3390/en10060803.
- [11] M. R. Al-Obaidi, W. Z. W. Hasan, M. A. Mustafa, and N. Aziz, "Charging Platform of Chess-Pad Configuration for Unmanned Aerial Vehicle (UAV)," *Applied Science MDPI*, vol. 10, no. 23, pp. 2-13, 2020, doi: 10.3390/app10238365.
- [12] Z. Huang, T. Zhang, P. Liu, and X. Lu, "Outdoor Independent Charging Platform System for Power Patrol UAV," *IEEE PES Asia-Pacific Power and Energy Engineering Conference (APPEEC)*, 2020, pp. 1-5, doi: 10.1109/APPEEC48164.2020.9220518.
- [13] M. C. Silverman, M. C., B. Jung, D. Nies and G. S. Sukhatme, "Staying Alive Longer: Autonomous Robot Recharging Put to the Test," Centre for Robotics and Embedded Systems (CRES) Technical Report, University of Southern California: Los Angeles, CA, USA, 2003.
- [14] K. A. Swieringa *et al.*, "Autonomous battery swapping system for small-scale helicopters," in *IEEE International Conference on Robotics and Automation*, 2010, pp. 3335-3340, doi: 10.1109/ROBOT.2010.5509165.
- [15] P. K. Chittoor, B. Chokkalingam, and L. Mihet-Popa, "A Review on UAV Wireless Charging: Fundamentals, Applications, Charging Techniques and Standards," in *IEEE Access*, vol. 9, pp. 69235-69266, 2021, doi: 10.1109/ACCESS.2021.3077041.
- [16] N. X. Yin, S. Saat, S. H. Husin, Y. Yusop, and M. R. Awal, "The design of IPT system for multiple kitchen appliances using class E LCCL circuit," *International Journal of Electrical and Computer Engineering*, vol. 10, no. 4, pp. 3483-3491, 2020, doi: 10.11591/ijece.v10i4.pp3483-3491.
- [17] K. Aditya and S. S. Williamson, "Design considerations for loosely coupled inductive power transfer (IPT) system for electric vehicle battery charging-A comprehensive review," *IEEE Transportation Electrification Conference and Expo (ITEC)*, 2014, pp. 1-6, doi: 10.1109/ITEC.2014.6861764.
- [18] K. K. Hasan, S. Saat, Y. Yusop, H. Husin, and N. D. M. Sin, "The design of an efficient class E-LCCL capacitive power transfer system through frequency tuning method," *International Journal of Electrical and Computer Engineering*, vol. 11, no. 2, pp. 1095-1104, 2021, doi: 10.11591/ijece.v11i2.pp1095-1104.
- [19] M. K. Kazimierzczuk, *RF Power Amplifiers*. 2nd Edition, Wiley, 2014.
- [20] A. Ong, J. P. K. Sampath, G. F. H. Beng, T. YenKheng, D. M. Vilathgamuwa and N. X. Bac, "Analysis of impedance matched circuit for wireless power transfer," *40th Annual Conference of the IEEE Industrial Electronics Society*, 2014, pp. 2965-2970, doi: 10.1109/IECON.2014.7048931.
- [21] J. Kim and F. Bien, "Electric field coupling technique of wireless power transfer for electric vehicles," *IEEE Tencon-Spring*, 2013, pp. 267-271, doi: 10.1109/TENCONSpring.2013.6584453.
- [22] S. Masuda, T. Hirose, Y. Akihara, N. Kuroki, M. Numa and M. Hashimoto, "Impedance matching in magnetic-coupling-resonance wireless power transfer for small implantable devices," *IEEE Wireless Power Transfer Conference (WPTC)*, 2017, pp. 1-3, doi: 10.1109/WPT.2017.7953839.





- [23] S. W. Park, "Misaligned Effect and Exposure Assessment for Wireless Power Transfer System Using the Anatomical Whole-Body Human Model," *Progress in Electromagnetics Research C*, vol. 77, pp. 19–28, 2017, doi: 10.2528/PIERC17051909.
- [24] F. Kong, "Coil Misalignment Compensation Techniques for Wireless Power Transfer Links in Biomedical Implants," M.S. thesis, Electrical and Computer Engineering, The State University of New Jersey, 2015.
- [25] J. Li, L. Wang, and F. Yin, "Study on Series Printed-Circuit-Board Coil Matrix for Misalignment-Insensitive Wireless Charging," *IEEE Wireless Power Transfer Conference (WPTC)*, 2019, pp. 98–101, doi: 10.1109/WPTC45513.2019.9055701.

BIOGRAPHIES OF AUTHORS







Khairul Kamarudin Hasan     is currently working with School of Electrical Engineering, College of Engineering, Universiti Teknologi MARA Cawangan Johor, Kampus Pasir Gudang, Malaysia. He received the B. Eng in Electronic Engineering (Electronic Industrial) in 2012, the Msc. Eng degree in Electronic Engineering (System), in 2014 and Ph. D degree in Electronic Engineering from Technical University Malaysia Malacca in 2021. His research interest Wireless Power Transfer, Power Electronic, Control system and Drive. He can be contacted at email: khairul@uitm.edu.my.







Shakir Saat     was born in Kedah, Malaysia in 1981. He obtained his bachelor degree in Electrical Engineering from Universiti Teknologi Malaysia and Master in Electrical Engineering from the same university in 2002 and 2006, respectively. Furthermore, he obtained his PhD in Electrical Engineering from The University of Auckland in the field of nonlinear control theory in 2013. He started his carrier as a lecturer at Universiti Teknikal Malaysia Melaka in 2004 and he is now an Associate Professor of the same university. His research interest is on nonlinear systems control theory and wireless power transfer technologies. He has published one book (published by springer verlag) on polynomial control systems and more than 50 journals and mostly published in the high quality journal such as The Journal of the Franklin Institute, International Journal of Robust and Nonlinear Control, IET Control and etc. More than 30 conference papers have also been published and most of them are in the framework of nonlinear control theory and wireless power transfer technologies. He is also appointed as a reviewer for IEEE Transaction journals, The journal of system science, The Journal of the Franklin Institute, International Journal of Robust and Nonlinear Control, Circuit, systems and signal processing and many more. He can be contacted at email: shakir@utem.edu.my.



Yusmarnita Yusop     was born in Melaka, Malaysia in 1979. She received the B. Eng in Electrical Engineering (Mechatronic) from Universiti Teknologi Malaysia, in 2001, the M. Eng degree in Electrical Engineering from Kolej Universiti Tun Hussein Onn, Malaysia, in 2004 and Ph. D degree in Electrical Engineering (Capacitive Power Transfer) from Universiti Teknikal Malaysia Melaka in 2018. Her career as academician begins in 2005 as a Teaching Engineer at Department of Industrial Electronic, Technical University Malaysia Malacca and now she is a Senior Lecturer at the same university. Her area of research interests includes electronic system design, wireless power transfer and power electronics She can be contacted at email: yusmarnita@utem.edu.my.



Md Rabiul Awal     is currently working with School of Ocean Engineering, Universiti Malaysia Terengganu (UMT) as a lecturer. He has received his PhD in Communication Engineering from Universiti Malaysia Perlis (UniMAP), Malaysia, in 2018. He was awarded master's in computer science from International Islamic University Malaysia (IIUM), Malaysia and the B.Sc. in Electrical & Electronics Engineering from International Islamic University Chittagong (IIUC), Bangladesh and in 2015 and 2011 respectively. From 2011 to 2012, he worked as a RF Engineer in 3S Network (BD) Ltd. and from 2013 to 2015 he worked as research assistant in IIUM and UniMAP. His research interests include underwater communications, wireless power transfer and energy harvesting. He can be contacted at email: rabiulawal1@gmail.com.